

Bootstrapping leading hadronic muon anomaly

Ahmadullah Zahed

*ICTP, International Centre for Theoretical Physics,
Strada Costiera 11, 34135, Trieste, Italy.*

azahed@ictp.it

Abstract

We bootstrap the leading order hadronic contribution to muon anomalous magnetic moment. The leading hadronic contribution comes from the hadronic vacuum polarization function (HVP). We explore the bootstrap constraints, namely unitarity, analyticity, crossing symmetry and finite energy sum rules (FESR) from quantum chromodynamics (QCD). The unitarity appears as a positive semi-definite condition among the pion partial waves, form factor and spectral density function of HVP, which establishes a lower bound on leading order hadronic contribution to muon anomalous magnetic moment. We also impose chiral symmetry breaking to improve the bound slightly. By combining the lower bound with the remaining extensively calculated contributions, we achieve a bound on anomalous magnetic moment $a_\mu^{\text{bootstrap-min}} = 11659176.3_{-3}^{+3} \times 10^{-10}$ and standard model prediction saturates this bound within the error bars. We also present a possible improvement that is saturated by both lattice computation and measured value within the error bars.

Contents

1	Introduction	1
2	Bootstrapping leading hadronic contribution to muon anomaly	3
3	Improvement of FESRs inequalities	7
A	QCD finite energy sum rules	8

1 Introduction

The anomalous magnetic moment $a_\mu = (g - 2)_\mu/2$ of the muon encapsulates how the muon interacts with magnetic fields through its intrinsic spin. The measurements of the muon's magnetic moment [1, 2] show a deviation from theoretical prediction up to 5.0σ [3], while agreeing with lattice QCD simulations within 0.9σ [4, 5].

A significant contribution to this discrepancy arises from hadronic vacuum polarization (HVP) at the leading order in the fine-structure constant ($a_\mu^{\text{LO-HVP}}$), where the muon's interaction is influenced by the complex interplay of quarks and gluons through the strong force, as described by quantum

chromodynamics (QCD). The hadronic contribution is more elusive due to the strongly coupled, non-perturbative nature of QCD at low energies, unlike the electromagnetic contributions, which can be calculated with great precision. This makes the precise evaluation of the hadronic effects a central challenge to understand a_μ and its implications for particle physics.

The bootstrap approach in quantum field theory (QFT) is a non-perturbative framework utilizing basic principles like unitarity, analyticity, crossing and other symmetries of QFT to constrain theory space [6, 7].

This work provides a bootstrap approach to the hadronic contribution by imposing theoretical constraints. In particular, we use the fact that the imaginary part of HVP, pion partial wave and form factor satisfy semi-definite positivity due to unitarity [8]—see also [9]. Analyticity and crossing symmetry of pion amplitudes are used to compute the pion partial waves [10, 11]—see also [12–15]. We establish a lower bound on leading order hadronic contribution to muon anomalous magnetic moment using unitarity, analyticity, crossing symmetry and QCD finite energy sum rules (FESR). The theory of pions well approximates the low energy QCD due to chiral symmetry breaking. We use tree level χ PT to capture the low energy physics, which slightly improves the bound. Our lower bound is more robust than [16], where Holder’s inequality and FESRs were used to establish two-sided bounds.

The finite energy sum rules (FESR) have errors due to QCD parameters, mainly from gluon condensate $\langle\alpha G^2\rangle$, vacuum saturation constant¹ κ . Hence, we input FESRs as inequality up to a tolerance. The weakest choice of the tolerance is the error itself, which leads to the result from light quark contributions as 680.5_{-3}^{+3} and adding with charmonium and bottomonium resonance contributions [18], we reach our final bound $\text{Min}[a_\mu^{\text{LO-HVP}}] = 688.4_{-3}^{+3} \times 10^{-10}$ and combining with other precisely calculated standard model(SM) contributions [3], we find

$$a_\mu^{\text{bootstrap-min}} = 11659176.3_{-3}^{+3} \times 10^{-10}, \quad (1)$$

while the measured value is $a_\mu^{\text{exp}} = 11659208.9_{-6.3}^{+6.3} \times 10^{-10}$. The prediction from the SM is [3] $a_\mu^{\text{SM}} = 11659181.0_{-4.3}^{+4.3} \times 10^{-10}$. The SM prediction within the error bars saturates our lower bound.

The improvement due to the tolerance is evident from the fact that the probability of finding the mean value is greater, and the QCD parameters $\langle\alpha G^2\rangle$ and κ are poorly determined. Since FESRs are equalities, we don’t want these inequalities too far away from the mean value. Choosing the tolerance as half of the error gives the result from light quark contributions as $707.5_{-1.6}^{+1.6}$ and adding with charmonium and bottomonium resonance contributions, we reach an improved lower bound $\text{Min}[a_\mu^{\text{LO-HVP}}] = 715.43_{-1.6}^{+1.6} \times 10^{-10}$ and adding with other extensively calculated SM contributions [3], we find

$$a_\mu^{\text{bootstrap-min-improved}} = 11659203.3_{-1.6}^{+1.6} \times 10^{-10}. \quad (2)$$

This is incompatible with SM prediction while saturated² by lattice evaluation [5] $a_\mu^{\text{lattice}} = 11659201.9(3.8) \times 10^{-10}$ and measured value within the error bars. Figure (1) summarises our findings.

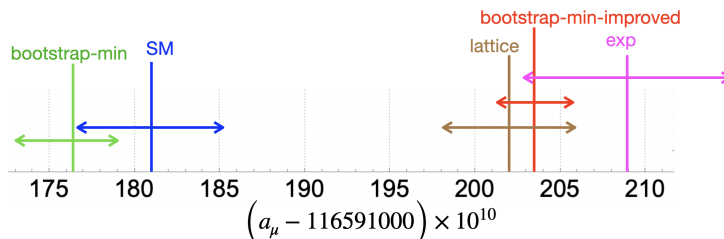


Figure 1: Comparison: SM prediction (dark blue) within the error bars saturates our conservative lower bound (green). However, an improved bound (red) is incompatible with SM prediction and is saturated by the lattice result (brown) and within the error bars of the measured value (magenta).

¹The proportionality constant that expresses dimension-six quark condensates as products of dimension-three quark condensates, $\alpha_s \langle(\bar{n}n)^2\rangle = \kappa \alpha_s \langle\bar{n}n\rangle^2$ [17].

²The bootstrap solution for the improved lower bound corresponds to $\langle\alpha G^2\rangle = 0.06315 \text{ GeV}^4$, $\kappa = 3.47$, while known literature values are $0.0649 \pm 0.0035 \text{ GeV}^4$, 3.22 ± 0.5 , respectively—see tables in appendix (A). Assuming that the theory of nature saturates the lower bound, the agreement of improved lower bound with lattice and measured value suggests that these are the potential numbers for $\langle\alpha G^2\rangle$, κ .

2 Bootstrapping leading hadronic contribution to muon anomaly

The leading hadronic contribution to muon anomalous magnetic moment is given by

$$a_\mu^{\text{LO-HVP}} = \frac{4\alpha^2}{\pi} \int_{4m_\pi^2}^{\infty} \frac{K(t)\text{Im}\Pi(t)}{t} dt, \quad (3)$$

where $\Pi(t) = \sum_{q=u,d,s} e_q^2 \Pi_q(t)$ is the hadronic vacuum polarization (HVP) and Π_q are contributions from different quarks. The kernel is given by $K(t) = \int_0^1 dx \frac{x^2(1-x)}{x^2+(1-x)t/m_\mu^2}$. The $\text{Im}\Pi(t)$ is proportional to the hadronic R-ratio. We will set $m_\pi = 1$ for convenience. We use unitarity condition on $\text{Im}\Pi(t)$ along with analyticity and FESRs to bootstrap $a_\mu^{\text{LO-HVP}}$.

Following [8], we write down the unitarity condition among imaginary part of HVP, pion partial wave and form factor as positive semi-definite condition

$$B(s) \equiv \begin{pmatrix} 1 & S_1^1(s) & \mathcal{F}_1^1(s) \\ S_1^{1*}(s) & 1 & \mathcal{F}_1^{1*}(s) \\ \mathcal{F}_1^{1*}(s) & \mathcal{F}_1^1(s) & \rho_1^1(s) \end{pmatrix} \succeq 0, \quad s > 4. \quad (4)$$

The rescaled spectral functions are given by $\rho_1^1(s) \times \frac{(2\pi)^4}{s} = \text{Im}\Pi(s)$ and $\mathcal{F}_1^1(s) = \frac{\sqrt{\frac{4\pi}{3}(\frac{s-4}{4})^{3/4}}}{(8\pi^3)^{1/4}\sqrt{s}} F(s)$, where $F(s)$ is some vector form factor normalized such that $F(0) = 1$. Further, S_1^1 is the spin-1 pion partial wave for the anti-symmetric sector. This unitarity condition is a generalization of Watson's equation [19]. For derivation and details³, we refer to [8, 9]. The FESRs for each quark contribution $\int_4^{s_0} \text{Im}\Pi_q(t) t^k dt, k = 0, 1, 2$ are well known [16, 20, 21]. One can add each quark contribution with appropriate pre-factors to write FESRs for $\int_4^{s_0} t^n \rho_1^1(t)$.

Bootstrap strategy: Impose unitarity condition (4), analyticity, sum rules for $\int_4^{s_0} t^n \rho_1^1(t)$ and partial wave unitarity $|S_\ell^I(s)| \leq 1$ to scan the space of $S_\ell^I(s)$, $\rho_1^1(s)$ and $\mathcal{F}_1^1(s)$ which minimizes $a_\mu^{\text{LO-HVP}}$.

We also impose chiral symmetry breaking, which marginally improves the bound.

2.1 Bootstrap implementations

In this section, we show the details of the numerical implementation of the bootstrap. We write a suitable ansatz for the pion partial waves, form factor and spectral density.

The pion partial waves $S_\ell^I(s) = 1 + i\pi \sqrt{\frac{s-4}{s}} f_\ell^I(s)$ are given by

$$f_\ell^I(s) = \frac{1}{4} \int_{-1}^1 dx P_\ell(x) M^{(I)} \left(s, t = \frac{(s-4)(x-1)}{2} \right), \quad (5)$$

where the isospin I channel amplitudes are

$$\begin{aligned} M^{(0)} &= 3A(s|t, u) + A(t|s, u) + A(u|t, s), \\ M^{(1)} &= A(t|s, u) - A(u|t, s), \\ M^{(2)} &= A(t|s, u) + A(u|t, s). \end{aligned} \quad (6)$$

The crossing symmetry and analyticity of $A(s|t, u)$ implies the following ansatz [10],

$$A(s|, t, u) = \sum_{n=1}^P \sum_{m=1}^n a_{nm} (\eta_t^m \eta_u^n + \eta_t^n \eta_u^m) + \sum_{n=0}^P \sum_{m=0}^P b_{nm} (\eta_t^m + \eta_u^m) \eta_s^n, \quad (7)$$

³Keeping in mind $J_\mu = \sum_{q=u,d,s} e_q \bar{q} \gamma_\mu q$.

where $\eta_z = \frac{(\sqrt{4-4/3}-\sqrt{4-z})}{(\sqrt{4-4/3+\sqrt{4-z}})}$ and we truncate the sum upto P . The analyticity of spectral density and form factor implies the following ansatz [8],

$$\rho_1^1(s) = - \sum_{n=1}^N d_n \sin \left(n \arccos \left(\frac{8}{s} - 1 \right) \right), \quad F(s) = \sum_{n=0}^N b_n \left(\frac{\sqrt{4} - \sqrt{4-s}}{\sqrt{4} + \sqrt{4-s}} \right)^n. \quad (8)$$

Note that $b_0 = 1$ because of $F(s=0) = 1$.

After writing down the ansatz, we want to impose FESRs for $\int_4^{s_0} t^n \rho_1^1(t)$ when $n = -1, 0, 1$. The choice of the s_0 is crucial. The lower the value of s_0 , the better, the lower bound, as was pointed out in [16]. However we can't go arbitrarily low in s_0 . Below $s_0 = 1.19$ GeV, the strange quark FESRs starts violating simple positivity inequality derived from Holder's inequality [16]. Hence, we stop at $s_0 = 1.19$ GeV –see appendix for details. The FESRs, along with the errors coming from the QCD parameters

$$\begin{aligned} \frac{1}{s_0} \int_4^{s_0} \frac{\rho_1^1(t)}{t} &= 0.0000416772_{-0.00000000105807}^{+0.00000000260880}, \\ \frac{1}{s_0^2} \int_4^{s_0} \rho_1^1(t) &= 0.0000186454 \pm 6.4034 \times 10^{-8}, \\ \frac{1}{s_0^3} \int_4^{s_0} t \rho_1^1(t) &= 9.17113 \times 10^{-6} \pm 5.6487 \times 10^{-7}. \end{aligned} \quad (9)$$

The sum rules are given in the appendix⁴. The dimension-four gluon condensate $\langle \alpha G^2 \rangle$, vacuum saturation constant (κ) provide dominant contributions to the errors [16]. For the convenience of determining tolerance, we considered an error for the first sum rule coming from strange quark mass, even though it has no visible effect in numerics.

Since the FESRs have errors, we naively can't put them as equality. Rather, we must put them as inequality upto a tolerance. A weak but rigorous possible choice for the tolerance is the error, namely (mean – error) $< \frac{1}{s_0^{2+n}} \int_4^{s_0} t^n \rho_1^1(t) < (\text{mean} + \text{error})$. Considering this, we have

$$\begin{aligned} 0.0000416667 &< \frac{1}{s_0} \int_4^{s_0} \frac{\rho_1^1(t)}{t} < 0.0000417033, \\ 0.0000185063 &< \frac{1}{s_0^2} \int_4^{s_0} \rho_1^1(t) < 0.0000187844, \\ 8.51123 \times 10^{-6} &< \frac{1}{s_0^3} \int_4^{s_0} t \rho_1^1(t) < 9.81765 \times 10^{-6}. \end{aligned} \quad (10)$$

An improvement of the tolerance will be discussed in the upcoming section. Given the ansatz, now we are in a position to minimize $a_\mu^{\text{LO-HVP}}$ imposing the constraints (4), (10) and partial wave unitarity $|S_\ell^I(s)| \leq 1$.

2.2 Step by step bootstrap

We illustrate the bootstrap implementation in three steps. Firstly, we consider the simplest bootstrap constraint between form factor and spectral density. The result from the first step is comparable to known literature. In the second step, we consider the full bootstrap conditions and increasing partial wave unitary constraints spin by spin. Thirdly, we consider chiral symmetry breaking, which improves the numerics slightly.

Step 1 \ Simplest condition for form factor and spectral density

Unitary condition (4) implies that all the principle minors of the matrix $B(s)$ are non-negative, resulting in a simple condition $\rho_1^1(s) \geq |\mathcal{F}_1^1(s)|^2$ upon considering the bottom-right minor. Solely

⁴These calculations should be done carefully considering the RG running for α_s and condensates. I thank the authors of [16] for helping us to reproduce their results. The details are in the appendix.

using this condition and FESRs (10), it is possible to achieve a minimum for $a_\mu^{\text{LO-HVP}}$ as demonstrated in figure (2). The extrapolation⁵ for large number of basis elements (N) gives $\text{Min}[a_\mu^{\text{LO-HVP}}] = 630.7_{-3}^{+3} \times 10^{-10}$.

A comparison: A reasonable comparison for the number $\text{Min}[a_\mu^{\text{LO-HVP}}] = 630.7_{-3}^{+3} \times 10^{-10}$ can be found in [16]. In [16], a two-sided bound on $a_\mu^{\text{LO-HVP}}$ was derived using positivity of the spectral density and FESRs for each quark section utilizing Holder's inequalities. For lower bound, the authors noticed that simple form of Kernel $K(t)$ enables to write $a_\mu^{\text{LO-HVP}} \geq 0.83 \times \frac{4\alpha^2 m_\mu^2}{3\pi} \times \int_{4m_\pi^2}^\infty \frac{\text{Im}\Pi(t)}{t^2}$ and FESRs puts a lower bound on $\int_{4m_\pi^2}^\infty \frac{\text{Im}\Pi(t)}{t^2}$. Considering errors for FESRs coming from gluon condensate $\langle \alpha G^2 \rangle$, vacuum saturation constant (κ) they arrive at conclusion that $a_\mu^{\text{LO-HVP}} > 657_{-34}^{+34} \times 10^{-10}$. Since we are using FESRs as inequalities due to errors and minimization process picks up the lowest of the bound, hence correct number we should compare is $a_\mu^{\text{LO-HVP}} > 623 \times 10^{-10}$, which is in good agreement with our lower bound $\text{Min}[a_\mu^{\text{LO-HVP}}] = 630.7_{-3}^{+3} \times 10^{-10}$ achieved using simplest condition $\rho_1^1(s) \geq |\mathcal{F}_1^1(s)|^2$ and FESRs.

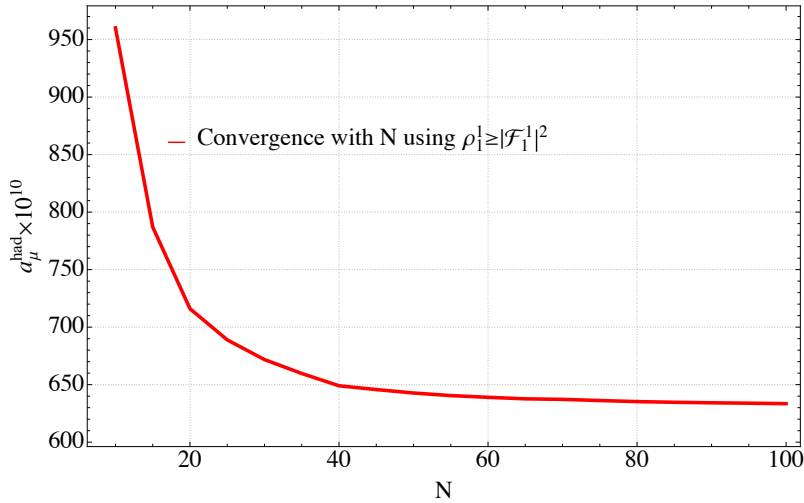


Figure 2: Convergence of numerics with the number of basis elements N for the simplest condition $\rho_1^1(s) \geq |\mathcal{F}_1^1(s)|^2$.

Step 2\ Comprehensive constraints for form factor, spectral density and partial waves

We now focus on complete numerics after demonstrating a simple form of numerics and a successful comparison. We implement the condition (4) by converting the $B(s)$ matrix into a 6×6 matrix [8] with

an equivalent condition $\begin{pmatrix} \text{Re}B(s) & -\text{Im}B(s) \\ \text{Im}B(s) & \text{Re}B(s) \end{pmatrix} \succeq 0$ using SDPB solver [23]. We impose the partial

wave unitarity $|S_\ell^I(s)| \leq 1$ upto spin L , namely $\ell = 1, 3, 5, \dots, L$ for isospin $I = 1$ and $\ell = 0, 2, 4, \dots, L-1$ for $I = 0, 2$. We remind the reader that truncation in the number of basis elements is N in eq (8) and P in eq (7). Convergence⁶ with N, L, P are shown in figure (3). Truncating the spin at $L = 9$ and $P = 10$ does not alter the third significant digits. Hence, throughout our analysis, we use these truncations. The convergence with N is evident in figure (3). For light quark contribution, the final bound in second step is $680.0_{-3}^{+3} \times 10^{-10}$, which shows improvement from full unitarity.

Step 3\ Imposing chiral symmetry breaking

The theory of pion well approximates the low energy QCD due to chiral symmetry breaking. We use tree level χPT to capture the low energy physics. These barely improve the bound (adds half to the

⁵We do extrapolations for large N with different models and average the errors and mean values [22]. Since the convergence at the third significant digit is visible, we discarded the models that were far from these values.

⁶The minimum should stabilize at some point with N, L, P —see [6] for the primal bootstrap algorithm.

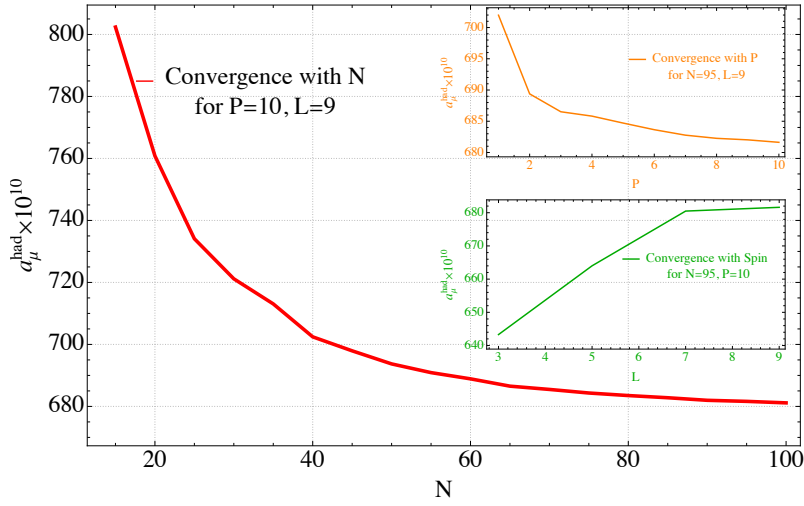


Figure 3: The convergence of numerics with N, L, P . We impose partial wave unitarity up to $\ell = 1, 3, 5, \dots L$ for isospin $I = 1$ and $\ell = 0, 2, 4, \dots L - 1$ for isospin $I = 0, 2$, P is the truncation of the sum for ansatz for $A(s|t, u)$ in (7) and N is the truncation in (8).

third significant digit), but we impose these for completeness. The tree-level partial waves are

$$f_{0,\text{tree}}^0(s) = \frac{2}{\pi} \frac{2s-1}{32\pi f_\pi^2}, \quad f_{1,\text{tree}}^1(s) = \frac{2}{\pi} \frac{s-4}{96\pi f_\pi^2}, \quad f_{0,\text{tree}}^2(s) = \frac{2}{\pi} \frac{2-s}{32\pi f_\pi^2}. \quad (11)$$

For $0 \leq s \leq 4$, we impose the following

$$|f_0^0(s) - f_{0,\text{tree}}^0(s)| < 3 \times 10^{-2}, \quad |f_1^1(s) - f_{1,\text{tree}}^1(s)| < 3 \times 10^{-2}, \quad |f_0^2(s) - f_{0,\text{tree}}^2(s)| < 3 \times 10^{-2}. \quad (12)$$

We choose tolerance 3×10^{-2} , which is dictated by 2-loop answer that matches with the tolerance used in [9]. For example $f_{0,\text{tree}}^0$ differs maximum at $s = 4$ with 2-loop answer which is about 25%, hence we use tolerance of 30%. We impose these inequalities for $0 \leq s \leq 4$ with a spacing $1/2$. We observed that reducing the spacing to 1 does not change the answers to the 4th significant digits.

The convergence for the lower bound is shown in figure (4). The extrapolated value for large N is 680.5_{-3}^{+3} . Now adding with charmonium and bottomonium resonance contributions [18], we reach our final bound $\text{Min}[a_\mu^{\text{LO-HVP}}] = 688.4_{-3}^{+3} \times 10^{-10}$

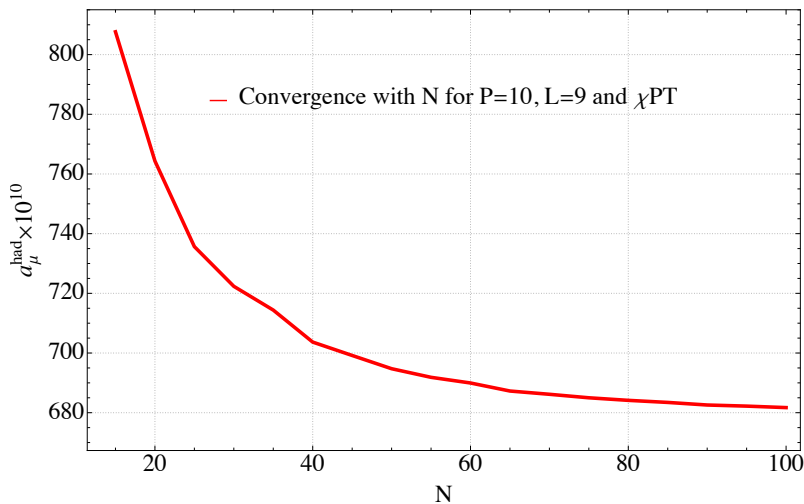


Figure 4: The convergence of numerics with N , the truncation in (8) imposing χ PT.

The upper bound does not converge. There is a transient plateau, which can be thought of as an upper bound; we refrain from showing the details.

2.3 Comparison with hadronic cross-ratio data

This section will compare extremal spectral density to the experimental hadronic cross-ratio data. We plot the $R(s) = 12\pi\text{Im}\Pi(s) = 12\pi \times \rho_1^1(s) \times \frac{(2\pi)^4}{s}$. For ρ -resonances appearing above $\sqrt{s} = 0.7$, bootstrap shows excellent agreement with the location of the peak in experimental hadronic cross-ratio data [24] –see figure (5). To demonstrate convergence, we plotted the bootstrapped data for

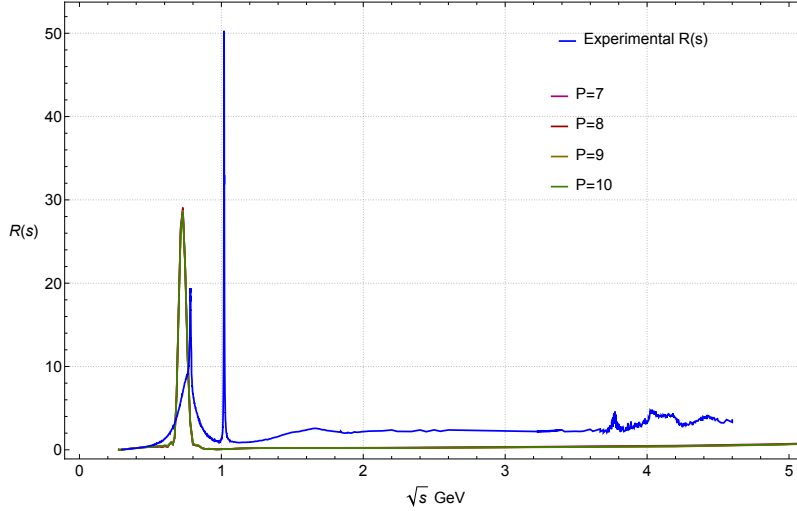


Figure 5: Comparison of bootstrap spectral density with the experimental hadronic cross ratio data. We find $m_\rho = 0.73$ GeV.

various P truncations with $L = 9, N = 95$. Data with or without imposing χ PT are almost identical. For these data, the peak position is about $\sqrt{s} = 0.73$, corresponding to ρ mass.

3 Improvement of FESRs inequalities

In this section, we discuss the improvement of the FESR inequalities. Improvement in tolerance is evident from the fact that the probability of finding the mean value is greater and the dimension-four gluon condensate $\langle\alpha G^2\rangle$, vacuum saturation constant (κ) are poorly determined amongst the QCD parameters. Since FESRs are equalities, we don't want these inequalities too far away from the mean value. We slightly improve the FESRs by choosing the tolerance as the half of the errors, namely $(\text{mean} - \frac{\text{error}}{2}) < \frac{1}{s_0^{2+n}} \int_4^{s_0} t^n \rho_1^1(t) < (\text{mean} + \frac{\text{error}}{2})$. Considering this, we have

$$\begin{aligned}
 0.00004167197 &< \frac{1}{s_0} \int_4^{s_0} \frac{\rho_1^1(t)}{t} < 0.0000416904, \\
 0.00001861338 &< \frac{1}{s_0^2} \int_4^{s_0} \rho_1^1(t) < 0.00001867741, \\
 8.888697 \times 10^{-6} &< \frac{1}{s_0^3} \int_4^{s_0} t \rho_1^1(t) < 9.453568 \times 10^{-6}.
 \end{aligned} \tag{13}$$

We show the convergence for the improved lower bound in figure (6). The extrapolation for large number of basis elements N gives $707.5_{-1.6}^{+1.6}$ and combining charmonium and bottomonium resonance contributions, we reach our improved bound $\text{Min}[a_\mu^{\text{LO-HVP}}] = 715.43_{-1.6}^{+1.6} \times 10^{-10}$.

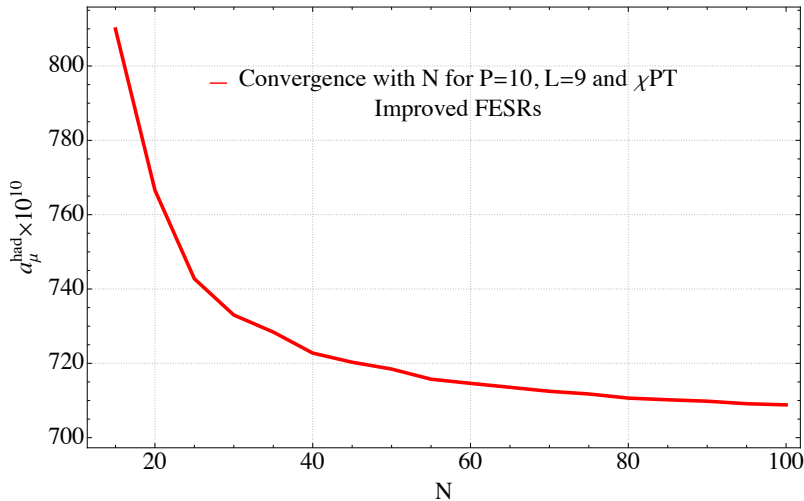


Figure 6: The convergence of numerics with N , the truncation in (8) considering χ PT and improved FESRs.

Discussion

We demonstrate that unitarity, analyticity, crossing symmetry and FESRs can establish a lower bound on $a_\mu^{\text{LO-HVP}}$. We demonstrate the bootstrap implementation in three steps. Firstly, we consider the simplest bootstrap constraint between form factor and spectral density and make a successful comparison to known literature. In the second step, we consider full bootstrap conditions and increasing partial wave unitary constraints spin by spin. Thirdly, we slightly improve the numerics by imposing chiral symmetry breaking. Adding $a_\mu^{\text{LO-HVP}}$ with rest of the extensively calculated SM contribution, we reach $a_\mu^{\text{bootstrap-min}} = 11659176.3_{-3}^{+3} \times 10^{-10}$, which saturated by SM prediction within the error bars. We compare bootstrap spectral density to the experimental hadronic cross-ratio data, which shows an excellent agreement. We also present a possible improvement of the FESRs, which gives an improved lower bound $a_\mu^{\text{bootstrap-min-improved}} = 11659203.3_{-1.6}^{+1.6} \times 10^{-10}$, which is incompatible with SM prediction while saturated by lattice evaluation and measured value within the error bars.

Acknowledgments

We thank Bobby Samir Acharya, Subham D. Chowdhury, Paolo Creminelli, Atish Dabholkar, Ehsan Ebrahimian, Aditya Hebbar, Joan Elias Miro, Andrea L. Guerrieri, Mehmet A. Gumus, Thomas G. Steele, Aninda Sinha, Shaswat Tiwari, and Alexander V. Zhiboedov for their helpful discussions. We would also like to thank SISSA, Trieste for supporting with their powerful clusters. I have received support from the European Research Council, grant agreement n. 101039756.

Appendix

A QCD finite energy sum rules

We use the following QCD sum rules

$$\begin{aligned}
\frac{1}{s_0} \int_4^{s_0} \frac{\rho_1^1(t)}{t} &= \frac{\pi}{s_0} \frac{1}{(2\pi)^4} \left(\frac{4}{9} F_0^{(up)}(s_0) + \frac{1}{9} F_0^{(down)}(s_0) + \frac{1}{9} F_0^{(strange)}(s_0) \right), \\
\frac{1}{s_0^2} \int_4^{s_0} \rho_1^1(t) &= \frac{\pi}{s_0^2} \frac{1}{(2\pi)^4} \left(\frac{4}{9} F_1^{(up)}(s_0) + \frac{1}{9} F_1^{(down)}(s_0) + \frac{1}{9} F_1^{(strange)}(s_0) \right), \\
\frac{1}{s_0^3} \int_4^{s_0} t \rho_1^1(t) &= \frac{\pi}{s_0^3} \frac{1}{(2\pi)^4} \left(\frac{4}{9} F_2^{(up)}(s_0) + \frac{1}{9} F_2^{(down)}(s_0) + \frac{1}{9} F_2^{(strange)}(s_0) \right),
\end{aligned} \tag{14}$$

with

$$F_0^{(q)}(s_0) = \frac{1}{4\pi^2} \left[1 + \frac{\alpha_s(\mu)}{\pi} T_{10} + \left(\frac{\alpha_s(\mu)}{\pi} \right)^2 (T_{20} + T_{21}) + \left(\frac{\alpha_s(\mu)}{\pi} \right)^3 (T_{30} + 2T_{31} + 2T_{32}) \right. \quad (15)$$

$$\left. + \left(\frac{\alpha_s(\mu)}{\pi} \right)^4 (T_{40} + 2T_{41} + 6T_{42} + 6T_{43}) \right] s_0 - \frac{3}{2\pi^2} m_q^2, \quad (16)$$

$$F_1^{(q)}(s_0) = \frac{1}{8\pi^2} \left[1 + \frac{\alpha_s(\mu)}{\pi} T_{10} + \left(\frac{\alpha_s(\mu)}{\pi} \right)^2 (T_{20} + T_{21}) + \left(\frac{\alpha_s(\mu)}{\pi} \right)^3 (T_{30} + T_{31} + T_{32}) \right. \quad (17)$$

$$\left. + \left(\frac{\alpha_s(\mu)}{\pi} \right)^4 \left(T_{40} + \frac{1}{3}T_{41} + \frac{2}{3}T_{42} + \frac{3}{4}T_{43} \right) \right] s_0^2 \quad (18)$$

$$- 2m_q \langle \bar{q}q \rangle \left(1 + \frac{\alpha_s(\mu)}{3} \right) - \frac{1}{12\pi} \langle \alpha_s G^2 \rangle \left(1 + \frac{7}{6} \frac{\alpha_s(\mu)}{\pi} \right), \quad (19)$$

$$F_2^{(q)}(s_0) = \frac{1}{12\pi^2} \left[1 + \frac{\alpha_s(\mu)}{\pi} T_{10} + \left(\frac{\alpha_s(\mu)}{\pi} \right)^2 \left(T_{20} + \frac{1}{3}T_{21} \right) + \left(\frac{\alpha_s(\mu)}{\pi} \right)^3 \left(T_{30} + \frac{1}{3}T_{31} + \frac{2}{9}T_{32} \right) \right. \quad (20)$$

$$\left. + \left(\frac{\alpha_s(\mu)}{\pi} \right)^4 \left(T_{40} + \frac{1}{3}T_{41} + \frac{2}{9}T_{42} + \frac{2}{9}T_{43} \right) \right] s_0^3 - \frac{224}{81} \pi \alpha_s(\mu) m_q \langle \bar{q}q q q \rangle, \quad (21)$$

where $\mu = \sqrt{s_0}$ and

$$F_k^{(q)}(s_0) = \int_{4m_\pi^2}^{s_0} \frac{\text{Im}\Pi_q(t)}{\pi} t^k dt \quad (22)$$

We numerically solve four loops RG equation for $\alpha_s(\mu)$ using $\alpha_s(M_\tau)$ as a boundary condition, which is above the charm threshold. Since we are interested in up to $s_0 = 1.19$ GeV, below the charm threshold, we start the RG for $N_f = 4$, do matching at the charm threshold, and then transit to $N_f = 3$. The RG equation is as follows [25]

$$\frac{1}{2} \mu \frac{\partial a(\mu)}{\partial \mu} = - \sum_{n=0}^3 a(\mu)^{n+2} \beta_n, \quad (23)$$

where $\alpha_s(\mu) = 4\pi a(\mu)$ with

$$\beta_0 = 11 - \frac{2}{3} N_f,$$

$$\beta_1 = 102 - \frac{38}{3} N_f,$$

$$\beta_2 = 1428.5 - 279.611 N_f + 6.01852 N_f^2,$$

$$\beta_3 = 29243 - 6946.3 N_f + 405.089 N_f^2 + 1.49931 N_f^3.$$

Leading order RG effect of quark mass is also taken care of [26]. RG effect for the condensates also has been take care of up to NLO using the fact that $m_q \langle \bar{q}q \rangle$ and $\langle \beta G^2 \rangle + 4\gamma m_q \langle \bar{q}q \rangle$ does not run with RG, where β is the beta function $\beta(\mu) = \mu \frac{\partial \alpha_s(\mu)}{\partial \mu}$ and γ is mass anomalous dimension $\mu \frac{\partial m_q(\mu)}{\partial \mu} = -\gamma(\mu) m_q(\mu)$.

We used QCD parameters as given below in tables (1), (2)–see [16] and references [17, 24–27],

Using Holder's inequality and positivity of $\text{Im}\Pi_q(t)$, the paper [16] established that each quark sector should obey the following inequality

$$\left(\frac{F_1}{(4m_\pi^2)^2} - F_B \right)^2 \leq \left(\frac{F_1}{(4m_\pi^2)^2} - F_0^2/F_1 \right)^2, \quad (24)$$

with $F_B = \frac{F_0}{4m_\pi^2} - \frac{\left(\frac{F_1}{4m_\pi^2} - F_0 \right)^2}{\frac{F_2}{4m_\pi^2} - F_1}$ and we have suppressed the q, s_0 labels from $F_k^{(q)}(s_0)$ for clarity. One can easily verify that for up and down quark, it gets violated below $s_0 = 1.09$ GeV while for strange quark, it gets violated below $s_0 = 1.19$ GeV–see [16].

Coefficient	Value
T_{10}	1
T_{20}	1.63982
T_{21}	$\frac{9}{4}$
T_{30}	-10.2839
T_{31}	11.3792
T_{32}	$\frac{81}{16}$
T_{40}	-106.896
T_{41}	-46.2379
T_{42}	47.4048
T_{43}	$\frac{729}{64}$

Table 1: Coefficients for $N_f = 3$.

Parameter	Value
α	1/137.036
$\alpha_s(M_\tau)$	0.312 ± 0.015
$m_u(2 \text{ GeV})$	$2.16^{+0.49}_{-0.26} \text{ MeV}$
$m_d(2 \text{ GeV})$	$4.67^{+0.48}_{-0.17} \text{ MeV}$
$m_s(2 \text{ GeV})$	$0.0934^{+0.0086}_{-0.0034} \text{ GeV}$
f_π	$(0.13056 \pm 0.00019)/\sqrt{2} \text{ GeV}$
$m_n \langle \bar{n}n \rangle$	$-\frac{1}{2} f_\pi^2 m_\pi^2$
$m_s \langle \bar{s}s \rangle$	$r_m r_c m_n \langle \bar{n}n \rangle$
r_c	0.66 ± 0.10
$m_s/m_n = r_m$	$27.33^{+0.67}_{-0.77}$
$\langle \alpha G^2 \rangle (2 \text{ GeV})$	$0.0649 \pm 0.0035 \text{ GeV}^4$
κ	3.22 ± 0.5
$\kappa \alpha_s \langle \bar{n}n \rangle^2$	$\kappa (1.8 \times 10^{-4}) \text{ GeV}^6$
$\alpha_s \langle (\bar{s}s)^2 \rangle$	$r_c^2 \alpha_s \langle \bar{n}n \rangle^2$

Table 2: QCD parameters and values with $m_n = (m_u + m_d)/2$, $\langle \bar{n}n \rangle = \langle \bar{u}u \rangle = \langle \bar{d}d \rangle$.

References

- [1] D. P. Aguillard *et al.* [Muon g-2], “Measurement of the Positive Muon Anomalous Magnetic Moment to 0.20 ppm,” Phys. Rev. Lett. **131** (2023) no.16, 161802 doi:10.1103/PhysRevLett.131.161802 [arXiv:2308.06230 [hep-ex]].
- [2] D. P. Aguillard *et al.* [Muon g-2], “Detailed report on the measurement of the positive muon anomalous magnetic moment to 0.20 ppm,” Phys. Rev. D **110** (2024) no.3, 032009 doi:10.1103/PhysRevD.110.032009 [arXiv:2402.15410 [hep-ex]].
- [3] T. Aoyama, N. Asmussen, M. Benayoun, J. Bijnens, T. Blum, M. Bruno, I. Caprini, C. M. Carloni Calame, M. Cè and G. Colangelo, *et al.* “The anomalous magnetic moment of the muon

- in the Standard Model,” *Phys. Rept.* **887** (2020), 1-166 doi:10.1016/j.physrep.2020.07.006 [arXiv:2006.04822 [hep-ph]].
- [4] S. Borsanyi, Z. Fodor, J. N. Guenther, C. Hoelbling, S. D. Katz, L. Lellouch, T. Lippert, K. Miura, L. Parato and K. K. Szabo, *et al.* “Leading hadronic contribution to the muon magnetic moment from lattice QCD,” *Nature* **593** (2021) no.7857, 51-55 doi:10.1038/s41586-021-03418-1 [arXiv:2002.12347 [hep-lat]].
- [5] A. Boccaletti, S. Borsanyi, M. Davier, Z. Fodor, F. Frech, A. Gerardin, D. Giusti, A. Y. Kotov, L. Lellouch and T. Lippert, *et al.* “High precision calculation of the hadronic vacuum polarisation contribution to the muon anomaly,” [arXiv:2407.10913 [hep-lat]].
- [6] M. Kruczenski, J. Penedones and B. C. van Rees, “Snowmass White Paper: S-matrix Bootstrap,” [arXiv:2203.02421 [hep-th]].
- [7] D. Poland and D. Simmons-Duffin, “Snowmass White Paper: The Numerical Conformal Bootstrap,” [arXiv:2203.08117 [hep-th]].
- [8] D. Karateev, S. Kuhn and J. Penedones, “Bootstrapping Massive Quantum Field Theories,” *JHEP* **07** (2020), 035 doi:10.1007/JHEP07(2020)035 [arXiv:1912.08940 [hep-th]].
- [9] Y. He and M. Kruczenski, “Gauge Theory Bootstrap: Pion amplitudes and low energy parameters,” [arXiv:2403.10772 [hep-th]].
Y. He and M. Kruczenski, “Bootstrapping gauge theories,” [arXiv:2309.12402 [hep-th]].
- [10] A. L. Guerrieri, J. Penedones and P. Vieira, “Bootstrapping QCD Using Pion Scattering Amplitudes,” *Phys. Rev. Lett.* **122** (2019) no.24, 241604 doi:10.1103/PhysRevLett.122.241604 [arXiv:1810.12849 [hep-th]].
- [11] M. F. Paulos, J. Penedones, J. Toledo, B. C. van Rees and P. Vieira, “The S-matrix bootstrap. Part III: higher dimensional amplitudes,” *JHEP* **12** (2019), 040 doi:10.1007/JHEP12(2019)040 [arXiv:1708.06765 [hep-th]].
- [12] A. Bose, A. Sinha and S. S. Tiwari, “Selection rules for the S-Matrix bootstrap,” *SciPost Phys.* **10** (2021) no.5, 122 doi:10.21468/SciPostPhys.10.5.122 [arXiv:2011.07944 [hep-th]].
A. Bose, P. Haldar, A. Sinha, P. Sinha and S. S. Tiwari, “Relative entropy in scattering and the S-matrix bootstrap,” *SciPost Phys.* **9** (2020), 081 doi:10.21468/SciPostPhys.9.5.081 [arXiv:2006.12213 [hep-th]].
- [13] J. Elias Miro, A. L. Guerrieri and M. A. Gumus, “Extremal Higgs couplings,” *Phys. Rev. D* **110** (2024) no.1, 016007 doi:10.1103/PhysRevD.110.016007 [arXiv:2311.09283 [hep-ph]].
- [14] A. Sinha and A. Zahed, “Crossing Symmetric Dispersion Relations in Quantum Field Theories,” *Phys. Rev. Lett.* **126** (2021) no.18, 181601 doi:10.1103/PhysRevLett.126.181601 [arXiv:2012.04877 [hep-th]].
- [15] A. Zahed, “Positivity and geometric function theory constraints on pion scattering,” *JHEP* **12** (2021), 036 doi:10.1007/JHEP12(2021)036 [arXiv:2108.10355 [hep-th]].
- [16] S. Li, T. G. Steele, J. Ho, R. Raza, K. Williams and R. T. Kleiv, “QCD bounds on leading-order hadronic vacuum polarization contributions to the muon anomalous magnetic moment,” *Phys. Rev. D* **110** (2024) no.1, 014046 doi:10.1103/PhysRevD.110.014046 [arXiv:2404.08591 [hep-ph]].
- [17] D. Harnett, J. Ho and T. G. Steele, “Correlations Between the Strange Quark Condensate, Strange Quark Mass, and Kaon PCAC Relation,” *Phys. Rev. D* **103** (2021) no.11, 114005 doi:10.1103/PhysRevD.103.114005 [arXiv:2104.00752 [hep-ph]].
- [18] A. Keshavarzi, D. Nomura and T. Teubner, “ $g - 2$ of charged leptons, $\alpha(M_Z^2)$, and the hyperfine splitting of muonium,” *Phys. Rev. D* **101** (2020) no.1, 014029 doi:10.1103/PhysRevD.101.014029 [arXiv:1911.00367 [hep-ph]].
- [19] K. M. Watson, “Some general relations between the photoproduction and scattering of pi mesons,” *Phys. Rev.* **95** (1954), 228-236 doi:10.1103/PhysRev.95.228
- [20] M. A. Shifman, A. I. Vainshtein and V. I. Zakharov, “QCD and Resonance Physics. Theoretical Foundations,” *Nucl. Phys. B* **147** (1979), 385-447 doi:10.1016/0550-3213(79)90022-1

- [21] M. A. Shifman, A. I. Vainshtein and V. I. Zakharov, “QCD and Resonance Physics: Applications,” Nucl. Phys. B **147** (1979), 448-518 doi:10.1016/0550-3213(79)90023-3
- [22] A. Guerrieri, J. Penedones and P. Vieira, “Where Is String Theory in the Space of Scattering Amplitudes?,” Phys. Rev. Lett. **127** (2021) no.8, 081601 doi:10.1103/PhysRevLett.127.081601 [arXiv:2102.02847 [hep-th]].
- [23] D. Simmons-Duffin, “A Semidefinite Program Solver for the Conformal Bootstrap,” JHEP **06** (2015), 174 doi:10.1007/JHEP06(2015)174 [arXiv:1502.02033 [hep-th]].
- [24] R. L. Workman *et al.* [Particle Data Group], “Review of Particle Physics,” PTEP **2022** (2022), 083C01 doi:10.1093/ptep/ptac097
[Link for hadronic cross ratio data.](#)
- [25] T. van Ritbergen, J. A. M. Vermaseren and S. A. Larin, “The Four loop beta function in quantum chromodynamics,” Phys. Lett. B **400** (1997), 379-384 doi:10.1016/S0370-2693(97)00370-5 [arXiv:hep-ph/9701390 [hep-ph]].
- [26] J. Gasser and H. Leutwyler, “Quark Masses,” Phys. Rept. **87** (1982), 77-169 doi:10.1016/0370-1573(82)90035-7
- [27] P. A. Baikov, K. G. Chetyrkin and J. H. Kuhn, “Order $\alpha^4(s)$ QCD Corrections to Z and tau Decays,” Phys. Rev. Lett. **101** (2008), 012002 doi:10.1103/PhysRevLett.101.012002 [arXiv:0801.1821 [hep-ph]].
M. R. Ahmady, F. A. Chishtie, V. Elias, A. H. Fariborz, D. G. C. McKeon, T. N. Sherry, A. Squires and T. G. Steele, “Optimal renormalization group improvement of the perturbative series for the $e^+ e^-$ annihilation cross-section,” Phys. Rev. D **67** (2003), 034017 doi:10.1103/PhysRevD.67.034017 [arXiv:hep-ph/0208025 [hep-ph]].
M. Gell-Mann, R. J. Oakes and B. Renner, “Behavior of current divergences under $SU(3) \times SU(3)$,” Phys. Rev. **175** (1968), 2195-2199 doi:10.1103/PhysRev.175.2195
R. Albuquerque, S. Narison and D. Rabetiariivony, “Scrutinizing the light scalar quarkonia from LSR at higher orders,” Nucl. Phys. A **1039** (2023), 122743 doi:10.1016/j.nuclphysa.2023.122743 [arXiv:2305.02421 [hep-ph]].